S100A8 and S100A9 Mediate Endotoxin-Induced Cardiomyocyte Dysfunction via the Receptor for Advanced Glycation End Products

John H. Boyd, Bernard Kan, Haley Roberts, Yingjin Wang, Keith R. Walley

Abstract—Cardiovascular dysfunction as a result of sepsis is the leading cause of death in the critically ill. Cardiomyocytes respond to infectious pathogens with a Toll-like receptor–initiated proinflammatory response in conjunction with a decrease in contractility, although the downstream events linking Toll-like receptor activation and reduced cardiac contractility remain to be elucidated. Using microarray analysis of cardiac tissue exposed to systemic lipopolysaccharide (LPS), we discovered that 2 small calcium-regulating proteins (S100A8 and S100A9) are highly upregulated. HL-1 cardiomyocytes, isolated primary cardiomyocytes, and live mice were exposed to LPS, whereas beating HL-1 cells had S100A8 and S100A9 overexpressed and their calcium flux quantified. Using in vivo microbubble technology, we delivered S100A8 and S100A9 to normal mouse hearts; using the same technology, we inhibited S100A9 production in mouse hearts and subsequently exposed them to LPS. Coimmunoprecipitation of S100A8 and S100A9 identified interaction with RAGE (the receptor for advanced glycation end products), the cardiac function and postreceptor signaling of which were investigated. HL-1 cardiomyocytes, isolated primary cardiomyocytes, and whole hearts exposed to LPS have large increases in S100A8 and S100A9. Cardiac overexpression of S100A8 and S100A9 led to a RAGE-dependent decrease in calcium flux and, in the intact mouse, to a decreased cardiac ejection fraction, whereas knockdown of S100A9 attenuated LPS-induced cardiac dysfunction. Cardiomyocytes exposed to LPS express S100A8 and S100A9, leading to a RAGE-mediated decrease in cardiomyocyte contractility. This finding provides a novel mechanistic link between circulating pathogen-associated molecular products and subsequent cardiac dysfunction. (***Circ Res*****. 2008;102:1239-1246.)**

Key Words: S100 proteins ■ RAGE ■ ventricular contractility

Sepsis causes myocardial dysfunction, which contributes to hypotension, impaired perfusion, and even death.[1] The precise mechanisms linking sepsis to myocardial dysfunction are still unclear; however, it is known that the function of cardiomyocytes extends beyond contraction to provide the motive force driving cardiac output and arterial pressure generation. There is increasing evidence that cardiomyocytes have additional properties, analogous in some respects to innate immune antigen-presenting cells that allow cardiomyocytes to respond to "danger" signals with an innate immune inflammatory and functional response.[2–23] We have recently shown that cardiomyocytes express multiple Toll-like receptors (TLRs) that signal predominantly through NF-κB when stimulated by pathogenic molecules, resulting in decreased cardiomyocyte contractility.[24] However, the downstream elements that link TLRs and cardiomyocyte contractility remain unknown. Because decreased contractility can be observed in isolated cardiomyocytes, we searched for candidate molecules that are highly regulated by exposure to TLR ligands and are capable of either exerting an autocrine effect and/or interacting with key intracellular contractile proteins. Using microarray analysis of cardiac tissue following systemic challenge with the TLR ligand lipopolysaccharide (LPS), we identified 2 small calcium-binding proteins (S100A8 and S100A9) as being highly upregulated in cardiomyocytes as early as 6 hours after LPS exposure.

S100A8 and S100A9 are members of the EF-hand family of proteins, in which the S100 proteins comprises the largest subfamily. S100 proteins are known to be important to heart function: S100A1 is a key mediator of contractile performance and overexpression of myocardial S100A1 leads to increased contractility[25] and improved performance after myocardial infarction,[26] whereas S100 A1 knockout mice exhibit features of congestive heart failure.[27] S100A1 exerts its positive effect on calcium flux and contractility via interaction with and potentiation of sarcoplasmic reticulum Ca^{2+}-ATPase (SERCA2a) and the ryanodine receptor (RyR)2.[25–35] Although S100A1 has been identified as an important therapeutic target, to date, there is little information

Original received November 8, 2007; revision received March 25, 2008; accepted March 31, 2008.

From the Critical Care Research Laboratories, St. Paul's Hospital, University of British Columbia, Vancouver, Canada.

Correspondence to John H. Boyd, MD, Critical Care Research Laboratories, 1081 Burrard St, Vancouver, BC, Canada V6Z 1Y6. E-mail jboyd@mrl.ubc.ca

about members of the S100 family being functionally present in the heart during inflammation or sepsis.

Unique among EF-hand proteins, S100A8 and S100A9 are found in both the intracellular and extracellular spaces[36–38] and, therefore, could potentially act both within the cell and in an autocrine manner. In immune cells, S100A8 and S100A9 are known to be upregulated and secreted in inflammatory conditions,[36–40] leading to signaling via RAGE (receptor for advanced glycation end products) to induce chemotaxis of neutrophils and amplify the proinflammatory cascade.[41] In addition to this outside-in signaling, given the high degree of homology between the members of the S100 family,[42] it is possible that S100A8 and S100A9 interact with 1 or more of the calcium-regulating proteins SERCA2a and RyR2 to exert an intracellular effect on cardiomyocyte contractility.

We, therefore, hypothesized that cardiomyocytes produce S100A8 and S100A9 in response to exposure to LPS. Given their dual intra- and extracellular roles, we also hypothesized that there would be separate extracellular (RAGE-dependent) and intracellular (RAGE-independent) effects on cardiac contractility.

Materials and Methods

Cell Line

HL-1 cells are an immortalized cell line with adult cardiac morphological, biochemical, and electrophysiological properties, including contraction and biochemical response to cognate ligands.[43] Stimulations and transfections were performed with the cells at confluence.

Primary Murine Cardiomyocytes

Murine ventricular myocytes were isolated from 10- to 14-week-old adult male mice. Isolation was performed as previously described.[24]

Cardiac-Specific Gene Delivery

We altered previously published methods of ultrasound guided gene therapy[44–49] using commercially available reagents and confirming cardiac delivery in preliminary experiments using LacZ as a marker.

Echocardiographic Assessment of Mice

Mice were lightly anesthetized with 1% to 3% inhaled isoflurane and placed on a warming blanket. M-mode echocardiograms were targeted from 2D echoes obtained using the Vevo 770 ECHO (Visualsonics, Toronto, Ontario, Canada) operating at a 120-Hz frame rate.

Statistical Analysis

All values were expressed as means±SE. For each experimental condition and time point, 4 independent replicate analyses were performed, unless otherwise noted. ANOVA and the post hoc Bonferroni test were used to identify specific differences between groups. The analyses were performed using Sigmastat (SPSS, Chicago, Ill), and statistical significance was set at $P<0.05$.

An expanded Materials and Methods section is available in the online data supplement at http://circres.ahajournals.org.

Results

Systemic Treatment With LPS Results in Reduced Cardiac Ejection Fraction and Is Associated With a Large Increase in Left Ventricular S100A8 and S100A9

Adult male mice were injected IP with 40 mg/kg *Escherichia coli*–derived LPS, and cardiac function was assessed preinjection (baseline) and at 6 hours after LPS by echocardiography. Baseline cardiac ejection fraction was 76%, falling to 29% 6 hours following injection of LPS (Figure 1A). Left ventricular tissue was harvested immediately following echocardiography at 6 hours, and quantitative RT-PCR revealed a 42-fold increase in S100A8 and a 49-fold increase in S100A9 mRNA compared with saline-treated mice (Figure 1B).

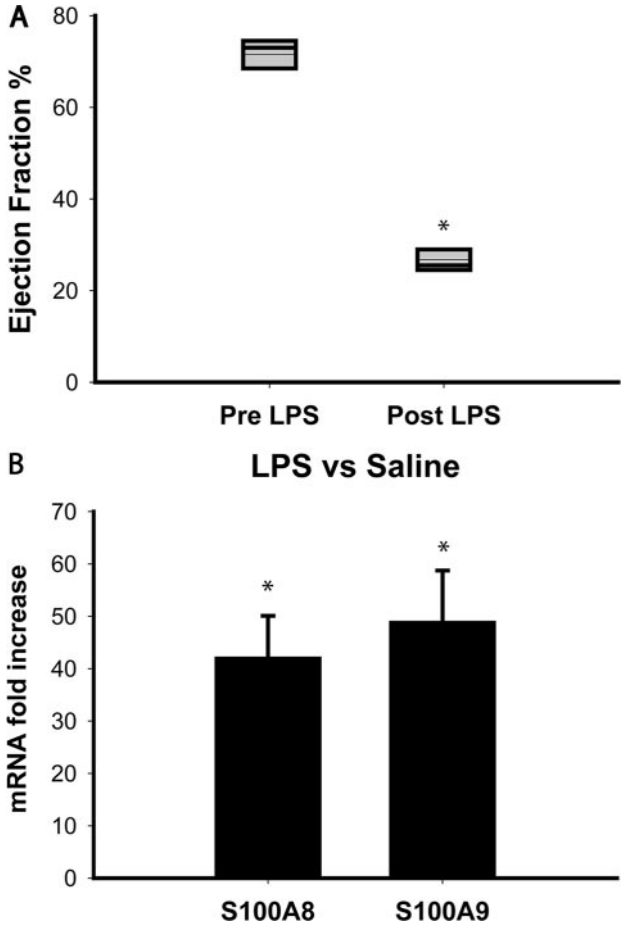

Figure 1. Eight- to 10-week old male C57BL/6 mice were injected IP with 40 mg/kg LPS. A, Cardiac ejection fraction was measured before and 6 hours after injection, demonstrating a dramatic drop in EF following LPS administration. B, mRNA from left ventricular tissue was analyzed by quantitative RT-PCR for S100A8 and S100A9 and compared with levels in mice injected with saline. Dramatic increases in left ventricular S100A8 and S100A9 are seen in mice exposed to LPS. *$P<0.05$ vs control.

S100A8 and S100A9 Are Constitutively Found in the HL-1 Cardiac Cell Line, Primary Cardiomyocytes, and Cardiac Tissue; Both Proteins Are Upregulated Following Exposure to LPS

To confirm that cardiomyocytes, rather than nonmyocyte cardiac cells, were responsible for cardiac S100A8 and S100A9 production, immunoblotting was performed on protein lysates from HL-1 cardiomyocytes, primary isolated cardiomyocytes, and left ventricular cardiac tissue exposed to either saline or LPS. All 3 groups had low levels of S100A8 and S100A9 constitutively expressed (saline-treated),

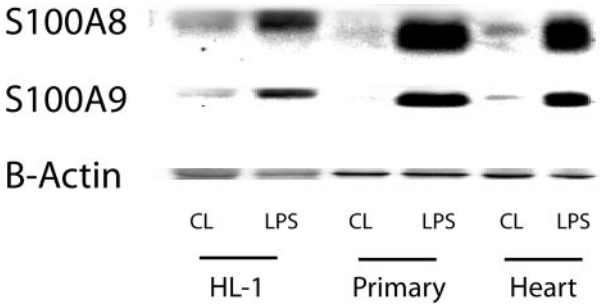

Figure 2. To confirm that S100A8 and S100A9 are expressed at the protein level and that the cells that express them are cardiomyocytes, immunoblotting was performed on protein lysates from HL-1 cardiomyocytes and isolated primary cardiomyocytes treated overnight with saline or 10 μg/mL LPS. Mice injected IP with 40 mg/kg LPS had hearts excised at 6 hours and were compared with animals injected with saline. In HL-1 cardiomyocytes, isolated primary cardiomyocytes, and heart tissue, there was a detectable but low constitutive level of S100A8 and S100A9, whereas LPS induced strong expression in all 3. CL indicates control.

whereas exposure to LPS resulted in increased S100A8 and S100A9 expression in all 3 groups (Figure 2).

Production of S100A8 and S100A9 in Cardiomyocytes Exposed to LPS Is Dependent on MyD88 and Partially Dependent on NF-κB

To determine the pathways responsible for LPS-induced production of S100A8 and S100A9, we used genetically altered mice deficient in the major pathways downstream from TLRs. Because TLR signaling is generally divided into MyD88-dependent or MyD88-independent, we chose to examine whether this adaptor protein was necessary for S100 protein production. In wild-type mice, LPS treatment resulted in a large increase in cardiac S100A8 and S100A9 production, whereas MyD88-null mice had no detectable production of either protein (Figure 3A and 3B). NF-κB is among the major downstream targets of MyD88, and is the predominant pathway in early inflammatory signaling. We found that NF-κB–deficient mice had increased S100A8/A9 production in response to LPS; however, this increase was significantly attenuated when compared with the response observed in wild-type mice (Figure 3A and 3B).

S100A8 and S100A9 Both Result in Decreased Cardiomyocyte Calcium Flux

HL-1 cells beat spontaneously in a concentric fashion, and, therefore, usual measures of contractility, such as fractional shortening, are not able to be reliably performed. However, it is well documented that the HL-1 cardiac action potential, as measured by either patch-clamp or calcium-gated fluorescence, mirrors the expected cardiac contractile response when exposed to cognate cardiac ligands.[50] We assessed the effect of S100A8 and S100A9 on cardiac contractility by measuring calcium flux in HL-1 cells transfected with plasmids encoding cDNA from 1 or both and compared these cells to those transfected with a control plasmid (LacZ). S100A8, S100A9, and both together resulted in a significant decrease in calcium flux compared with control vector (Figure 4A and 4B).

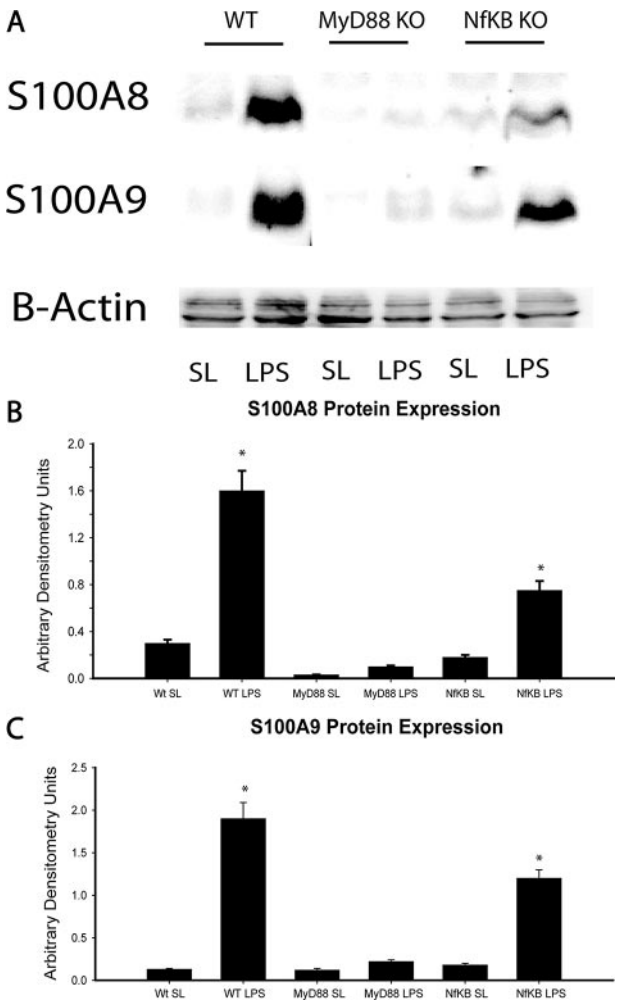

Figure 3. Eight- to 10-week-old male mice that were injected IP with 40 mg/kg LPS had hearts excised at 6 hours and were compared with animals injected with saline (SL). The major signaling pathways involved in signaling following exposure to LPS were examined in relation to S100A8 and -A9 production through the use of knockout mice (MyD88 and NF-κB). A, Representative Western blot. B, Group mean densitometry data from multiple mice. Wild-type (WT) mice have strong induction of both S100A8 and S100A9 following injection with LPS, whereas MyD88 knockout (KO) mice have near-total inhibition of this response. NF-κB knockout mice had a significantly blunted response. *$P<0.05$ vs saline.

Cardiac Delivery of S100A8 and S100A9 In Vivo Results in Decreased Ejection Fraction; Knockdown of S100A9 Abrogates LPS-Induced Cardiac Dysfunction

We used small animal echocardiography combined with lipid microbubbles carrying endotoxin-free plasmids to deliver S100A8 and S100A9 or both to the murine heart in vivo. As demonstrated in Figure 5A through 5C, by day 2, there was a strong trend toward decreased cardiac contractility in mice given cardiac S100A8, S100A9, or both compared with control plasmid, although only S100A9 reached statistical significance. All 3 groups demonstrated significant decreases in cardiac ejection fraction compared with control plasmid by day 5.

In separate mice, we determined whether S100A9 has a role in LPS-induced cardiac dysfunction. One week before LPS injection, cardiac-specific delivery of S100A9 small

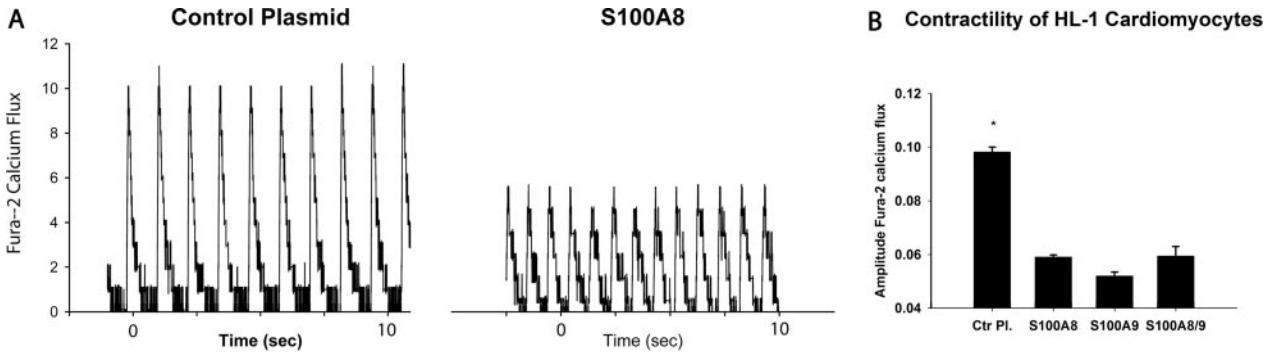

Figure 4. Spontaneously beating HL-1 cardiomyocytes were transfected with plasmids encoding S100A8, S100A9, S100A8+A9, or LacZ (Control). Calcium flux as measured by Fura-2 fluorescence is taken after 24 hours. A, Representative traces showing cells transfected with control plasmid or S100A8 are shown with a large reduction in calcium flux in cells expressing S100A8. B, Group mean data showing large and statistically significant reductions in calcium flux in beating HL-1 cells transfected with S100A8, S100A9, and both S100A8 and -A9 compared with control. *$P<0.05$ vs control (Ctr).

interfering (si)RNA was performed, and ejection fraction was measured before and 6 hours after LPS (Figure 5D). Mice that had received control plasmid had a 35% reduction in cardiac ejection fraction compared with a 12% reduction in mice in which S100A9 production in response to LPS was reduced by half (Figure 5D).

Coimmunoprecipitation Reveals a Physical Interaction Between RAGE and Cardiac S100A8 and S100A9

Because S100A8 and S100A9 are secreted and interact with the RAGE receptor in other cell types, we next determined whether cardiac S100A8 or S100A9 interacted with the cardiac RAGE receptor. C57BL/6 mice were injected IP with 40 mg/kg LPS to upregulate S100A8 and S100A9. Six hours after injection, hearts were excised and digested to obtain isolated cardiac myocytes. Coimmunoprecipitation was performed with anti-S100A8, anti-S100A9, or nonspecific IgG, and the immunoprecipitate was then probed with anti-RAGE antibody. We found that RAGE coimmunoprecipitated with both S100A8 and S100A9, demonstrating a strong interaction between the RAGE receptor and these proteins (Figure 6).

S100A8 and S100A9 Decrease Cardiomyocyte Calcium Flux and Induce NF-κB via the Transmembrane RAGE Receptor

Given that S100A8 and S100A9 physically interact with RAGE on cardiomyocytes (Figure 6), we next determined whether this interaction was responsible for the decrease in cardiac contrac-

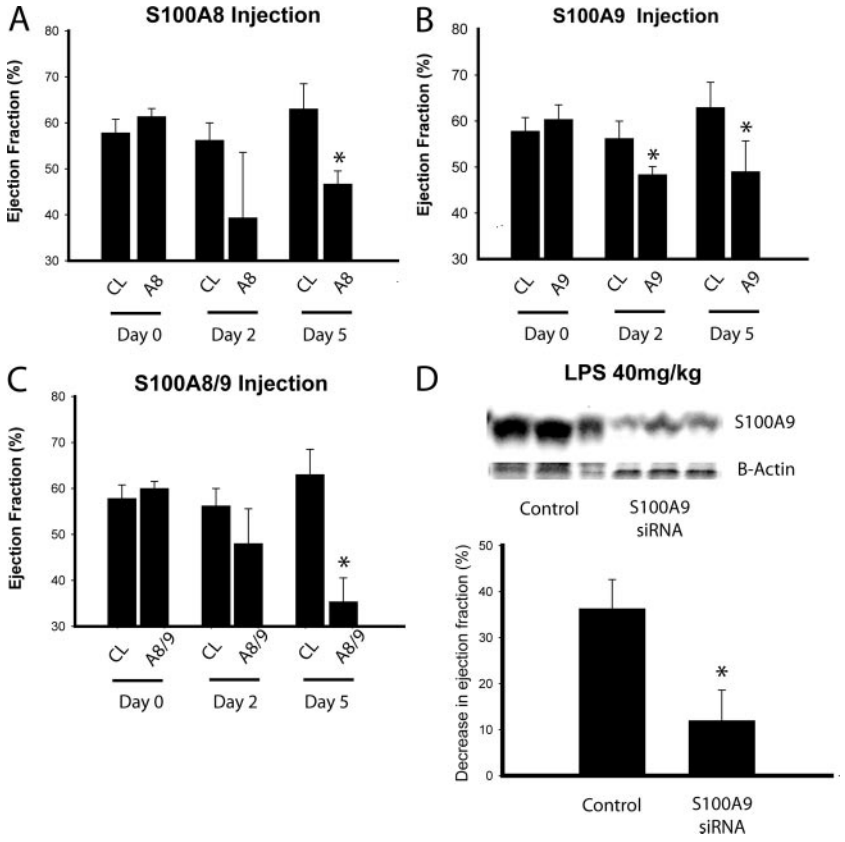

Figure 5. A through C, Eight- to 10-week-old male C57BL/6 mice had cardiac specific gene delivery of S100A8, S100A9, S100A8+A9, or control plasmid. By day 5 after injection, all 3 groups demonstrated significant decreases in cardiac ejection fraction vs control plasmid. D, Eight- to 10-week-old male C57BL/6 mice had cardiac-specific gene delivery of a plasmid encoding 3 siRNA sequences to S100A9 or scrambled sequences (CL), then, at 1 week, were injected with 40 mg/kg LPS. Immunoblotting heart digests for S100A9 at 6 hours after LPS treatment revealed a 47% attenuation in cardiac S100A9 production in mice pretreated with S100A9 siRNA compared with mice pretreated with scrambled siRNA. Mice that received control siRNA had a 37% decrease in cardiac ejection fraction at 6 hours compared with only 12% in mice treated with S100A9 siRNA. *$P<0.05$ vs control.

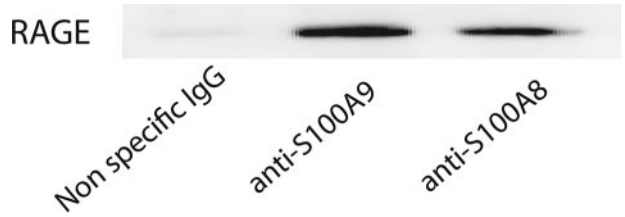

Figure 6. Eight- to 10-week-old male C57BL/6 mice were injected IP with 40 mg/kg LPS to upregulate S100A8 and S100A9. At 6 hours after injection, hearts were excised and digested to obtain isolated cardiac myocytes. Coimmunoprecipitation was performed with anti-S100A8, anti-S100A9, or nonspecific IgG. The immunoprecipitate was then probed with anti-RAGE antibody, demonstrating a strong interaction between cardiac RAGE and both S100A8 and S100A9.

tility. Anti-RAGE blocking antibody was added before transfection of HL-1 cells with S100A8 and S100A9 and measurement of calcium flux. Surprisingly, blocking the RAGE receptor before transfection of S100A8 or S100A9 not only abolished the decrease in calcium flux but actually resulted in increased calcium flux compared with control cells (Figure 7A). Blocking RAGE in the absence of overexpressed S100A8 and S100A9 had no influence on calcium flux (Figure 7A).

RAGE is known to signal predominantly through NF-κB in other cell types. We confirmed that S100A8 and S100A9 could induce NF-κB activity in HL-1 cardiomyocytes and that blocking RAGE abolished this signaling (Figure 7B).

Coimmunoprecipitation Reveals a Physical Interaction Between Cardiac S100A8, S100A9, and SERCA2a

We hypothesized that similar to S100A1, S100A8 and S100A9 may interact within the cardiomyocyte with 1 or both the calcium-regulating proteins SERCA2a and RyR2, leading to potentiation of the calcium flux. C57BL/6 mice were injected IP with 40 mg/kg LPS to upregulate S100A8 and S100A9. Six hours after injection, hearts were excised and digested to obtain isolated cardiac myocytes. Coimmunoprecipitation was performed with anti-S100A8, anti-S100A9, or nonspecific IgG. The immunoprecipitate was then probed with anti-SERCA2a and anti-RyR2 antibodies. We found that SERCA2a coimmunoprecipitated with both S100A8 and S100A9, demonstrating a strong interaction between SERCA2a and these proteins (Figure 8). No interaction was found between either S100A8 or S100A9 and RyR2 (data not shown).

Discussion

In this study, we propose a novel mechanistic link between activation of TLRs expressed on the surface of cardiomyocytes and the subsequent decrease in cardiac contractility.

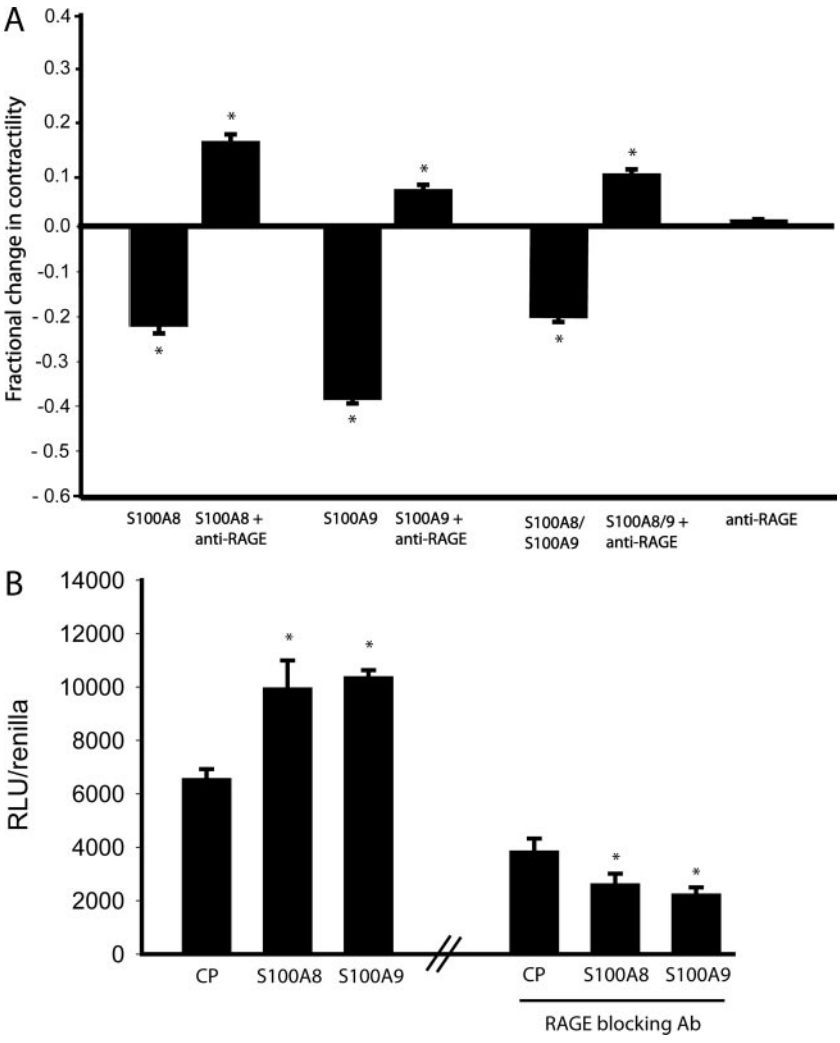

Figure 7. A, Spontaneously beating HL-1 cardiomyocytes were transfected with plasmids encoding S100A8, S100A9, S100A8+A9, or LacZ (control). The cells were then treated with blocking anti-RAGE antibody or isotype control. Calcium flux, as measured by Fura-2 fluorescence, was taken after 24 hours. HL-1 cells treated with nonspecific IgG demonstrated significantly reduced calcium flux in response to S100A8, S100A9, or both. In contrast, blockade of RAGE actually resulted in a significantly increased calcium flux in cells transfected with S100A8, S100A9, or both. RAGE blockade alone did not affect calcium flux. B, HL-1 cells were transfected with a plasmid containing a NF-κB–responsive promoter that activates transcription of firefly luciferase, as well as a constitutively active renilla–luciferase plasmid to control for transfection efficiency. They were cotransfected with either S100A8 or S100A9 and treated with blocking anti-RAGE antibody or isotype control. Both S100A8 and S100A9 strongly induce NF-κB, whereas blocking RAGE eliminated this response.

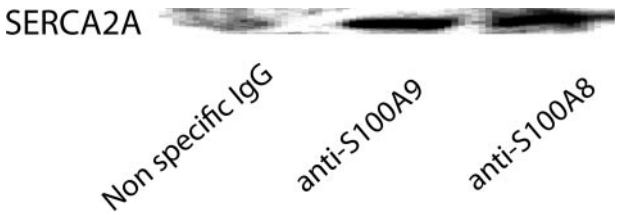

Figure 8. Eight- to 10-week-old male C57BL/6 mice were injected IP with 40 mg/kg LPS to upregulate S100A8 and S100A9. At 6 hours after injection, hearts were excised and digested to obtain isolated cardiac myocytes. Coimmunoprecipitation was performed with anti-S100A8, anti-S100A9, or nonspecific IgG. The immunoprecipitate was then probed with anti-SERCA2a antibody, demonstrating a strong interaction between cardiac SERCA2a and both S100A8 and S100A9.

The key finding in our study is that on stimulation with the bacterial product LPS, the EF-hand proteins S100A8 and S100A9 are upregulated in cardiomyocytes, leading to a RAGE-dependent decrease in cardiac contractility.

Although it has long been recognized that infection leads to abnormalities in cardiovascular function, the link between pathogen recognition and subsequent cardiac dysfunction remains unclear. We have recently shown that cardiomyocytes express multiple TLRs[24]; this family of receptors is thought to be responsible for innate immune recognition of pathogens and "self" danger molecules such as heat shock proteins. Following stimulation of these receptors with their cognate ligands, cardiomyocytes exhibit decreased contractility both in isolated preparations and in vivo.[24] Because TLRs are not known to interact with the cytoskeleton or contractile machinery, the link between TLR activation and subsequent cardiac contractile dysfunction is unlikely to be direct. Furthermore, because the effect on contractility persists in isolated cardiomyocytes, the pathways downstream of TLRs must lead to either an autocrine effect or interaction with key intracellular contractile proteins or both. With these criteria in mind, we used cDNA microarrays to identify S100A8 and S100A9, which are highly regulated by exposure of cardiomyocytes to TLR ligands. S100A8 and S100A9 are small EF-hand proteins that are capable of exerting both autocrine and intracellular effects.[42] Unique among the members of the S100 family, as well as the larger EF-hand superfamily, S100A8 and S100A9 are found not only intracellularly but also in the extracellular space.[36–38]

In this study, we show, for the first time, that exposure to the TLR4 ligand LPS causes an early, large upregulation of S100A8 and S100A9 expression in cardiomyocytes. This occurs both in whole heart tissue exposed to systemic LPS and in isolated cardiomyocytes exposed in vitro to LPS. Because it is extremely difficult in the intact heart to determine which type of cardiac cell is responsible for the production of any given molecule, the use of both systems affords a high degree of certainty that the origin of S100A8 and S100A9 is from cardiomyocytes. How does ligation of cardiomyocyte-expressed TLR4 result in the production of S100A8 and S100A9? TLRs are type I transmembrane receptors consisting of a variable number of extracellular leucine rich repeats linked to a cytoplasmic Toll/interleukin-1 receptor (TIR) homology domain.[51] Downstream signaling has been well characterized in TLRs and, although complex, can be divided into major pathways. Activation of most TLRs by ligand binding results in dimerization, a change in conformation, and recruitment of a variety of downstream signaling molecules.[52,53] All TLRs can signal via MyD88, and this pathway is considered to play a dominant role in early inflammatory events. MyD88 is recruited to the TIR domain of activated TLRs. MyD88 recruits IRAK-4, which activates IKK, leading to liberation of NF-κB from its inhibitor, IκBα, and subsequent translocation of NF-κB to the nucleus, where it induces proinflammatory cytokine production.[54,55] In addition to the MyD88-dependent pathway, alternative signaling pathways have been identified for TLR4. TLR4 induces interferon-β production independent of MyD88,[54] which induces STAT1 phosphorylation and proinflammatory gene expression.

Using MyD88 and NF-κB null mice, we determined that LPS-induced production of S100A8 and S100A9 is absolutely dependent on MyD88 and that, although NF-κB–null mice exhibited a greatly attenuated response to LPS, there remained a significant elevation of both S100A8 and S100A9. Given that MyD88-dependent signaling not involving NF-κB is through the mitogen-activated protein kinase (MAPK) cascade (p38 MAPK, extracellular signal-regulated kinase 1/2, and c-Jun N-terminal kinase),[56] it seems probable that LPS-induced S100A8 and S100A9 production is dependent on both NF-κB and MAPK. Interestingly, NF-κB and MAPK are also activated with overexpression of S100A8 and S100A9 in prostate cancer cells,[39] raising the possibility that a positive-feedback loop exists both upstream and downstream of S100A8 and S100A9.

We went on to show at both the cellular and the organ level that S100A8 and S100A9 reduce cardiomyocyte contractility, resulting in a reduced cardiac ejection fraction. We further showed that this reduction in contractility is through a RAGE-dependent mechanism. RAGE is a member of the immunoglobulin superfamily, with the extracellular portion of this cell surface receptor responsible for ligand binding.[57] Emerging as a key molecule responsible for diverse pathologies, including both vascular[58–61] and nonvascular conditions,[37,39,40,62] RAGE is a multiligand receptor known to bind advanced glycation end products (AGEs), amphoterin, amyloid β-peptide, and S100A8/S100A9.[61] AGEs have been the most studied ligand for RAGE, with particular interest in how this interaction may mediate macrovascular complications associated with hyperglycemia.[61] S100A8 and S100A9 are also known to activate RAGE and, depending on the cell type on which RAGE is expressed, can do so in either heterodimeric or homodimeric form.[37–40]

Extracellular cation flux, most notably Ca^{2+} and Zn^{2+}, induces conformational change and allows S100A8 and S100A9 to bind to RAGE, initiating signaling events within the cell. In immune cells, the interaction between S100A8/S100A9 and RAGE induces chemotaxis of neutrophils and secretion of proinflammatory cytokines.[41] In cardiomyocytes, ligation of RAGE by AGEs is known to impair cardiac

calcium flux[60] and has been shown to be a key mediator of both the proinflammatory state and contractile dysfunction associated with ischemia/reperfusion.[58] Our cardiomyocyte calcium flux and in vivo cardiac EF data suggest that the individual proteins (homodimeric) are capable of mediating reduced cardiac contractility, although it does appear in vivo that S100A8 combined with S100A9 reduces EF more than either given individually.

Although S100A8 and S100A9 do signal through RAGE under inflammatory conditions, with resultant decreased cardiac contractility, RAGE does not appear to have a constitutive effect on cardiomyocyte calcium flux because blocking RAGE under baseline conditions did not result in a change in calcium flux. However, when S100A8 and S100A9 are expressed with RAGE blocked, this resulted in significantly increased cardiomyocyte calcium flux. This augmented flux may reflect the high degree of homology between S100 proteins,[63] because S100A1 is known to exert a positive effect on calcium flux and contractility via interaction with, and potentiation of, the calcium-gating proteins SERCA2a and RyR2.[25–35] We went on to show through coimmunoprecipitation that both S100A8 and S100A9 do in fact physically interact with SERC2a, whereas no such interaction was found between them and RyR2.

These intriguing observations lead to the conclusion that S100A8 and S100A9 are not only immunologically active chemokines but are, in fact, important molecules with respect to cardiac function. They are produced by cardiomyocytes in response to inflammatory conditions and proceed to act in at least 2 compartments to influence cardiac contractility. The predominant effect is autocrine: extracellular interaction with cardiomyocyte-expressed RAGE results in decreased contractility. The second compartment is intracellular, where their physiological function is unmasked by blocking the more potent RAGE-mediated effects. Within the cell, cardiomyocyte calcium flux is potentiated by both S100A8 and S100A9, possibly through SERCA2a. This last function is speculative because, although our data suggest physical interaction, further investigations would be necessary to infer causation.

It is increasingly recognized that inflammation is a common underlying feature of many cardiac pathologies. TLRs recognize both invasive pathogens and, perhaps more importantly, endogenous markers of tissue damage, raising the strong possibility that this TLR-S100A8/A9 pathway is relevant to a host of inflammatory cardiac conditions such as ischemia, transplant rejection, and autoimmune disorders.

Sources of Funding

This work was supported by Canadian Institutes of Health Research. K.R.W. is a Michael Smith Foundation for Health Research Distinguished Scholar. J.H.B. is an IMPACT/Michael Smith Foundation for Health Research Postdoctoral Fellow and a Providence Health Research Institute Physician Scholar.

Disclosures

None.

References

1. Levy MM, Fink MP, Marshall JC, Abraham E, Angus D, Cook D, Cohen J, Opal SM, Vincent JL, Ramsay G. 2001 SCCM/ESICM/ACCP/ATS/SIS International Sepsis Definitions Conference. *Intensive Care Med*. 2003;29:530–538.
2. Goddard CM, Allard MF, Hogg JC, Walley KR. Myocardial morphometric changes related to decreased contractility after endotoxin. *Am J Physiol*. 1996;270:H1446–H1452.
3. Goddard CM, Poon BY, Klut ME, Wiggs BR, vanEeden SF, Hogg JC, Walley KR. Leukocyte activation does not mediate myocardial leukocyte retention during endotoxemia in rabbits. *Am J Physiol*. 1998;275:H1548–H1557.
4. Granton JT, Goddard CM, Allard MF, van Eeden S, Walley KR. Leukocytes and decreased left-ventricular contractility during endotoxemia in rabbits. *Am J Respir Crit Care Med*. 1977;155:1977–1983.
5. Herbertson MJ, Werner HA, Goddard CM, Russell JA, Wheeler A, Coxon R, Walley KR. Anti-tumor necrosis factor-alpha prevents decreased ventricular contractility in endotoxemic pigs. *Am J Respir Crit Care Med*. 1995;152:480–488.
6. Herbertson MJ, Werner HA, Russell JA, Iversen K, Walley KR. Myocardial oxygen extraction ratio is decreased during endotoxemia in pigs. *J Appl Physiol*. 1995;79:479–486.
7. Herbertson MJ, Werner HA, Studer W, Russell JA, Walley KR. Decreased left ventricular contractility during porcine endotoxemia is not prevented by ibuprofen. *Crit Care Med*. 1996;24:815–819.
8. Herbertson MJ, Werner HA, Walley KR. Nitric oxide synthase inhibition partially prevents decreased LV contractility during endotoxemia. *Am J Physiol*. 1996;270:H1979–84.
9. McDonald TE, Grinman MN, Carthy CM, Walley KR. Endotoxin infusion in rats induces apoptotic and survival pathways in hearts. *Am J Physiol Heart Circ Physiol*. 2000;279:H2053–H2061.
10. Simms MG, Walley KR. Activated macrophages decrease rat cardiac myocyte contractility: importance of ICAM-1-dependent adhesion. *Am J Physiol*. 1999;277:H253–H260.
11. Walley KR. Mechanics and energetics of tumor necrosis factor-alpha in the left ventricle. *Crit Care Med*. 1999;27:29–30.
12. Walley KR, Hebert PC, Wakai Y, Wilcox PG, Road JD, Cooper DJ. Decrease in left ventricular contractility after tumor necrosis factor-alpha infusion in dogs. *J Appl Physiol*. 1994;76:1060–1067.
13. Davani EY, Dorscheid DR, Lee CH, van Breemen C, Walley KR. Novel regulatory mechanism of cardiomyocyte contractility involving ICAM-1 and the cytoskeleton. *Am J Physiol Heart Circ Physiol*. 2004;287:H1013–H1022.
14. Brown MA, Jones WK. NF-kappaB action in sepsis: the innate immune system and the heart. *Front Biosci*. 2004;9:1201–1217.
15. De Rossi M, Bernasconi P, Baggi F, de Waal Malefyt R, Mantegazza R. Cytokines and chemokines are both expressed by human myoblasts: possible relevance for the immune pathogenesis of muscle inflammation. *Int Immunol*. 2000;12:1329–1335.
16. Figarella-Branger D, Civatte M, Bartoli C, Pellissier JF. Cytokines, chemokines, and cell adhesion molecules in inflammatory myopathies. *Muscle Nerve*. 2003;28:659–682.
17. Finkel MS, Oddis CV, Jacob TD, Watkins SC, Hattler BG, Simmons RL. Negative inotropic effects of cytokines on the heart mediated by nitric oxide. *Science*. 1992;257:387–389.
18. Hattori Y, Kasai K. Induction of mRNAs for ICAM-1, VCAM-1, and ELAM-1 in cultured rat cardiac myocytes and myocardium in vivo. *Biochem Mol Biol Int*. 1997;41:979–986.
19. Knuefermann P, Nemoto S, Misra A, Nozaki N, Defreitas G, Goyert SM, Carabello BA, Mann DL, Vallejo JG. CD14-deficient mice are protected against lipopolysaccharide-induced cardiac inflammation and left ventricular dysfunction. *Circulation*. 2002;106:2608–2615.
20. Lefer AM. Mechanisms of cardiodepression in endotoxin shock. *Circ Shock Suppl*. 1979;1:1–8.
21. Massey KD, Strieter RM, Kunkel SL, Danforth JM, Standiford TJ. Cardiac myocytes release leukocyte-stimulating factors. *Am J Physiol*. 1995;269:H980–H987.
22. Mehra VC, Ramgolam VS, Bender JR. Cytokines and cardiovascular disease. *J Leukoc Biol*. 2005;78:805–818.
23. Niessen HW, Krijnen PA, Visser CA, Meijer CJ, Hack CE. Intercellular adhesion molecule-1 in the heart. *Ann N Y Acad Sci*. 2002;973:573–585.
24. Boyd JH, Mathur S, Wang Y, Bateman RM, Walley KR. Toll-like receptor stimulation in cardiomyocytes decreases contractility and ini-

tiates an NF-kappaB dependent inflammatory response. *Cardiovasc Res*. 2006;72:384–393.
25. Most P, Remppis A, Pleger ST, Loffler E, Ehlermann P, Bernotat J, Kleuss C, Heierhorst J, Ruiz P, Witt H, Karczewski P, Mao L, Rockman HA, Duncan SJ, Katus HA, Koch WJ. Transgenic overexpression of the Ca2+-binding protein S100A1 in the heart leads to increased in vivo myocardial contractile performance. *J Biol Chem*. 2003;278:33809–33817.
26. Pleger ST, Remppis A, Heidt B, Volkers M, Chuprun JK, Kuhn M, Zhou RH, Gao E, Szabo G, Weichenhan D, Muller OJ, Eckhart AD, Katus HA, Koch WJ, Most P. S100A1 gene therapy preserves in vivo cardiac function after myocardial infarction. *Mol Ther*. 2005;12:1120–1129.
27. Most P, Seifert H, Gao E, Funakoshi H, Volkers M, Heierhorst J, Remppis A, Pleger ST, DeGeorge BR Jr, Eckhart AD, Feldman AM, Koch WJ. Cardiac S100A1 protein levels determine contractile performance and propensity toward heart failure after myocardial infarction. *Circulation*. 2006;114:1258–1268.
28. Kettlewell S, Most P, Currie S, Koch WJ, Smith GL. S100A1 increases the gain of excitation-contraction coupling in isolated rabbit ventricular cardiomyocytes. *J Mol Cell Cardiol*. 2005;39:900–910.
29. Most P, Bernotat J, Ehlermann P, Pleger ST, Reppel M, Borries M, Niroomand F, Pieske B, Janssen PM, Eschenhagen T, Karczewski P, Smith GL, Koch WJ, Katus HA, Remppis A. S100A1: a regulator of myocardial contractility. *Proc Natl Acad Sci U S A*. 2001;98:13889–13894.
30. Most P, Boerries M, Eicher C, Schweda C, Ehlermann P, Pleger ST, Loeffler E, Koch WJ, Katus HA, Schoenenberger CA, Remppis A. Extracellular S100A1 protein inhibits apoptosis in ventricular cardiomyocytes via activation of the extracellular signal-regulated protein kinase 1/2 (ERK1/2). *J Biol Chem*. 2003;278:48404–48412.
31. Most P, Pleger ST, Volkers M, Heidt B, Boerries M, Weichenhan D, Loffler E, Janssen PM, Eckhart AD, Martini J, Williams ML, Katus HA, Remppis A, Koch WJ. Cardiac adenoviral S100A1 gene delivery rescues failing myocardium. *J Clin Invest*. 2004;114:1550–1563.
32. Most P, Boerries M, Eicher C, Schweda C, Volkers M, Wedel T, Sollner S, Katus HA, Remppis A, Aebi U, Koch WJ, Schoenenberger CA. Distinct subcellular location of the Ca2+-binding protein S100A1 differentially modulates Ca2+-cycling in ventricular rat cardiomyocytes. *J Cell Sci*. 2005;118:421–431.
33. Pleger ST, Most P, Heidt B, Voelkers M, Hata JA, Katus HA, Remppis A, Koch WJ. S100A1 gene transfer in myocardium. *Eur J Med Res*. 2006;11:418–422.
34. Remppis A, Pleger ST, Most P, Lindenkamp J, Ehlermann P, Schweda C, Loffler E, Weichenhan D, Zimmermann W, Eschenhagen T, Koch WJ, Katus HA. S100A1 gene transfer: a strategy to strengthen engineered cardiac grafts. *J Gene Med*. 2004;6:387–394.
35. Volkers M, Loughrey CM, Macquaide N, Remppis A, DeGeorge BR Jr, Wegner FV, Friedrich O, Fink RH, Koch WJ, Smith GL, Most P. S100A1 decreases calcium spark frequency and alters their spatial characteristics in permeabilized adult ventricular cardiomyocytes. *Cell Calcium*. 2007;41:135–143.
36. Newton RA, Hogg N. The human S100 protein MRP-14 is a novel activator of the beta 2 integrin Mac-1 on neutrophils. *J Immunol*. 1998;160:1427–1435.
37. Huttunen HJ, Kuja-Panula J, Sorci G, Agneletti AL, Donato R, Rauvala H. Coregulation of neurite outgrowth and cell survival by amphoterin and S100 proteins through receptor for advanced glycation end products (RAGE) activation. *J Biol Chem*. 2000;275:40096–40105.
38. Hofmann MA, Drury S, Fu C, Qu W, Taguchi A, Lu Y, Avila C, Kambham N, Bierhaus A, Nawroth P, Neurath MF, Slattery T, Beach D, McClary J, Nagashima M, Morser J, Stern D, Schmidt AM. RAGE mediates a novel proinflammatory axis: a central cell surface receptor for S100/calgranulin polypeptides. *Cell*. 1999;97:889–901.
39. Hermani A, De Servi B, Medunjanin S, Tessier PA, Mayer D. S100A8 and S100A9 activate MAP kinase and NF-kappaB signaling pathways and trigger translocation of RAGE in human prostate cancer cells. *Exp Cell Res*. 2006;312:184–197.
40. Ehlermann P, Eggers K, Bierhaus A, Most P, Weichenhan D, Greten J, Nawroth PP, Katus HA, Remppis A. Increased proinflammatory endothelial response to S100A8/A9 after preactivation through advanced glycation end products. *Cardiovasc Diabetol*. 2006;5:6.
41. Ryckman C, Vandal K, Rouleau P, Talbot M, Tessier PA. Proinflammatory activities of S100: proteins S100A8, S100A9, and S100A8/A9 induce neutrophil chemotaxis and adhesion. *J Immunol*. 2003;170:3233–3242.
42. Fritz G, Heizmann CW. 3D structures of the calcium and zinc binding S100 proteins. In: Messerschmidt A, Bode W, Cygler M, eds. *Handbook of Metalloproteins*. Vol 3. Chichester, UK: Wiley; 2004:529–540.
43. Claycomb WC, Lanson NA Jr, Stallworth BS, Egeland DB, Delcarpio JB, Bahinski A, Izzo NJ Jr. HL-1 cells: a cardiac muscle cell line that contracts and retains phenotypic characteristics of the adult cardiomyocyte. *Proc Natl Acad Sci U S A*. 1998;95:2979–2984.
44. Bekeredjian R, Chen S, Frenkel PA, Grayburn PA, Shohet RV. Ultrasound-targeted microbubble destruction can repeatedly direct highly specific plasmid expression to the heart. *Circulation*. 2003;108:1022–1026.
45. Bekeredjian R, Chen S, Pan W, Grayburn PA, Shohet RV. Effects of ultrasound-targeted microbubble destruction on cardiac gene expression. *Ultrasound Med Biol*. 2004;30:539–543.
46. Bekeredjian R, Katus HA, Kuecherer HF. Therapeutic use of ultrasound targeted microbubble destruction: a review of non-cardiac applications. *Ultraschall Med*. 2006;27:134–140.
47. Bekeredjian R, Bohris C, Hansen A, Katus HA, Kuecherer HF, Hardt SE. Impact of microbubbles on shock wave-mediated DNA uptake in cells in vitro. *Ultrasound Med Biol*. 2007.
48. Korosoglou G, Behrens S, Bekeredjian R, Hardt S, Hagenmueller M, Dinjus E, Bohm KJ, Unger E, Katus HA, Kuecherer H. The potential of a new stable ultrasound contrast agent for site-specific targeting. An in vitro experiment. *Ultrasound Med Biol*. 2006;32:1473–1478.
49. Muller OJ, Katus HA, Bekeredjian R. Targeting the heart with gene therapy-optimized gene delivery methods. *Cardiovasc Res*. 2007;73:453–462.
50. White SM, Constantin PE, Claycomb WC. Cardiac physiology at the cellular level: use of cultured HL-1 cardiomyocytes for studies of cardiac muscle cell structure and function. *Am J Physiol Heart Circ Physiol*. 2004;286:H823–H829.
51. Akira S, Uematsu S, Takeuchi O. Pathogen recognition and innate immunity. *Cell*. 2006;124:783–801.
52. Slack JL, Schooley K, Bonnert TP, Mitcham JL, Qwarnstrom EE, Sims JE, Dower SK. Identification of two major sites in the type I interleukin-1 receptor cytoplasmic region responsible for coupling to pro-inflammatory signaling pathways. *J Biol Chem*. 2000;275:4670–4678.
53. Akira S, Takeda K. Toll-like receptor signalling. *Nat Rev Immunol*. 2004;4:499–511.
54. Akira S, Yamamoto M, Takeda K. Role of adapters in Toll-like receptor signalling. *Biochem Soc Trans*. 2003;31:637–642.
55. Palsson-McDermott EM, O'Neill LA. Signal transduction by the lipopolysaccharide receptor, Toll-like receptor-4. *Immunology*. 2004;113:153–162.
56. Oda K, Kitano H. A comprehensive map of the toll-like receptor signaling network. *Mol Syst Biol*. 2006;2:2006.0015.
57. Neeper M, Schmidt AM, Brett J, Yan SD, Wang F, Pan YC, Elliston K, Stern D, Shaw A. Cloning and expression of a cell surface receptor for advanced glycosylation end products of proteins. *J Biol Chem*. 1992;267:14998–15004.
58. Bucciarelli LG, Kaneko M, Ananthakrishnan R, Harja E, Lee LK, Hwang YC, Lerner S, Bakr S, Li Q, Lu Y, Song F, Qu W, Gomez T, Zou YS, Yan SF, Schmidt AM, Ramasamy R. Receptor for advanced-glycation end products: key modulator of myocardial ischemic injury. *Circulation*. 2006;113:1226–1234.
59. Kaneko M, Bucciarelli L, Hwang YC, Lee L, Yan SF, Schmidt AM, Ramasamy R. Aldose reductase and AGE-RAGE pathways: key players in myocardial ischemic injury. *Ann N Y Acad Sci*. 2005;1043:702–709.
60. Petrova R, Yamamoto Y, Muraki K, Yonekura H, Sakurai S, Watanabe T, Li H, Takeuchi M, Makita Z, Kato I, Takasawa S, Okamoto H, Imaizumi Y, Yamamoto H. Advanced glycation endproduct-induced calcium handling impairment in mouse cardiac myocytes. *J Mol Cell Cardiol*. 2002;34:1425–1431.
61. Yan SF, Ramasamy R, Naka Y, Schmidt AM. Glycation, inflammation, and RAGE: a scaffold for the macrovascular complications of diabetes and beyond. *Circ Res*. 2003;93:1159–1169.
62. Moser B, Szabolcs MJ, Ankersmit HJ, Lu Y, Qu W, Weinberg A, Herold KC, Schmidt AM. Blockade of RAGE suppresses alloimmune reactions in vitro and delays allograft rejection in murine heart transplantation. *Am J Transplant*. 2007;7:293–302.
63. Marenholz I, Heizmann CW, Fritz G. S100 proteins in mouse and man: from evolution to function and pathology (including an update of the nomenclature). *Biochem Biophys Res Commun*. 2004;322:1111–1122.

Circulation Research
JOURNAL OF THE AMERICAN HEART ASSOCIATION

S100A8 and S100A9 Mediate Endotoxin-Induced Cardiomyocyte Dysfunction via the Receptor for Advanced Glycation End Products

John H. Boyd, Bernard Kan, Haley Roberts, Yingjin Wang and Keith R. Walley

Circ Res. 2008;102:1239-1246; originally published online April 10, 2008;
doi: 10.1161/CIRCRESAHA.107.167544
Circulation Research is published by the American Heart Association, 7272 Greenville Avenue, Dallas, TX 75231

Print ISSN: 0009-7330. Online ISSN: 1524-4571

Materials and methods

Cell line: HL-1 cells are an immortalized cell line with adult cardiac morphological, biochemical, and electrophysiological properties, including contraction and biochemical response to cognate ligands. The cell line was kindly provided by Dr William Claycomb. Cells are grown in complete supplemented Claycomb media (JRH Biosciences, Lenexa, Kansas). Stimulations and transfections are performed with the cells at confluence.

Primary murine cardiomyocytes: Murine ventricular myocytes are isolated from 10-14 week old adult male mice. After pelleting, cells are suspended in AS media (Cellutron, Highland Park, NJ) at a density of 20,000 cells/mL and placed in a 37^{o}C incubator on matrigel (BD Biosciences, Franklin Lakes, NJ) coated coverslips. When cells are to be kept in culture greater than 8 hours 10 mM 2,3–butanedione monoxime is added to the media.

Genetically engineered mice: MyD88 knockout mice were obtained from S Quereshi (Montreal PQ). NF-κB knockout mice (NF-kB KO 129P-Nfkb1tm1Bal/J) were obtained from Jackson Labs. Genotype was verified through RT-PCR.

Cell culture treaments: 10ug/mL E. Coli LPS (Invivogen, San Diego CA) is added 4 hours prior to harvesting cells for RNA assays and, in separate experiments, 24 hours prior to harvesting supernatant for protein assays. Inhibition of RAGE**:** 1ug/ml anti-

murine RAGE blocking antibody (R&D Systems, Minneapolis MN) was added to supplemented Claycomb media + 10% FBS 24 hours prior to calcium flux measurement.

Plasmids and transfections: Lipofectamine 2000 in OPTIMEM (Invitrogen, Carlsbad, CA) is used as per the manufacturer's instructions. S100A8 and S100A9 vectors (Origene Technologies, Rockville, MD) and mock transfection using the backbone only is performed. We have found that transfection efficiency, as determined using a GFP containing plasmid, is 50-60% at 48 hours. S100A9 siRNA plasmid and control/scrambled siRNA plasmid (Sigma, Oakville Canada) were used in vivo only.

Luciferase assay: HL-1 cells were transfected as above using pNFkB-Luc vector (BD Biosciences, Franklin Lakes, NJ) and a Renilla pGL4.74 [hRluc/TK] vector (Promega, Madison, WI). Cells were lysed using Passive Lysis Buffer (Promega), then luminescence quantified using the Dual-Luciferase Reporter Assay (Promega #1910) and a Fluostar Optima Luminometer (BMG Labtech, Durham NC). Relative Light Units (RLU) were obtained for both Renilla and the Firefly Luciferase and all results expressed as the ratio of Luciferase RLU to Renilla RLU.

Immunoprecipitation and immunoblotting: Tissues and cells were were homogenized in cell lysis buffer containing protease inhibitors aprotinin 10 ug/uml and leupeptin 10ug/ml and the phosphatase inhibitor sodium orthovanadate 10 mM. Anti-S100A8 and anti-s100A9 (R&D Systems, Minneapolis MN), anti-RAGE (R&D Systems, Minneapolis MN) and anti-SERCA2A (Santa Cruz Biotech, Santa Cruz California) were used as

primary antibodies. Immunoprecipitation was performed with 1ug/ml anti-S100A8, S100A9 or isotype control Ab using the protein G immunoprecipitation kit (Roche, Laval PQ) as per the manufacturer's instructions.

Calcium flux assay: HL-1 cells grown to confluence on 4-well LabTek coverslips chambers (Sigma, Oakville, ON) are incubated for 30 minutes with 2.5 uM Fura-2 calcium-gated fluorescent dye (Molecular probes). Fluoresence is captured using a photomultiplier detector (Ionoptix corp, Milton, MA) and analyzed using an Ionoptix Softedge detection package that directly yields dynamic cardiomyocyte calcium flux (Ionoptix corp, Milton, MA). Calcium flux is calculated as peak to baseline difference in the ratio of emissions from excitation wavelengths 340/380 nm.

RNA extraction and quantitative RT-PCR: Total RNA is extracted using Trizol (Invitrogen, Carlsbad, CA) as per the manufacturer's instructions. 1 μg of RNA is treated with DNAase I Amplification Grade (Invitrogen, Carlsbad, CA). One step Quantitative real time RT-PCR will be performed using a SYBR green RT-PCR kit (QIAGEN Inc. Mississauga, ON) according to manufacture's instructions on an ABI 7200 detection system (Applied Biosystems, Foster City, CA). 20 μL samples are amplified using a program that includes a reverse transcription procedure consisting of one cycle at 50℃ for 30 minutes and 95℃ for 15 minutes followed by 40 cycles of denaturation step at 94 ℃ for 15 seconds, annealing step at 60℃ for 30 seconds and extension step at 72℃ for 30 seconds. The absolute amount of the target gene is determined using external

standards. S100A8 and S100A9 primers were obtained from ABI's list of pre-validated primer-probe sets (Applied Biosystems, Foster City, CA).

Cardiac-specific gene delivery: Depot microbubbles (Visualsonics, Toronto ON) 5uM in diameter are reconstituted with 2ug/ul endotoxin-free plasmid and incubated 30 minutes at room temperature. 4ul/gram of this plasmid-microbubble mixture is injected via mouse tail vein. Successful injection is confirmed through echocardiographic visualization with the Vevo 770 small animal ECHO (Visualsonics, Toronto ON) of contrast first in the right ventricular cavity then within 3 cardiac cycles the left ventricular cavity. Ten minutes following intravenous injection ventricular tissue opacification due to capillary lodging of the microbubbles is maximum while intravascular contrast has largely cleared. Microbubbles are then cavitated using 4 pulses per level of the low-frequency/high-energy "destruct" mode within the contrast software mode (Visualsonics, Toronto ON). This destruction is performed at levels from cardiac base to apex.

Echocardiographic assessment of mice: Mice are lightly anesthetized with 1-3% inhaled isofluorane and placed on a warming blanket. M-mode echocardiograms are targeted from 2D echos obtained using the Vevo 770 ECHO (Visualsonics, Toronto ON) operating at a 120 Hz frame rate. Left parasternal 2D left ventricular cross-sectional echocardiographic images are obtained. The position and angle of the echo transducer is maintained by directing the beam just off the tip of the anterior leaflet of the mitral valve and by maintaining internal anatomic landmarks constant. All measurements are taken from M-mode traces at end-expiration. Left ventricular internal dimensions will be

measured at end-diastole (defined as the onset of the QRS complex in lead II of the simultaneously obtained electrocardiogram) and at end-systole (defined as minimum internal ventricular dimension).

Materials and methods

Cell line: HL-1 cells are an immortalized cell line with adult cardiac morphological, biochemical, and electrophysiological properties, including contraction and biochemical response to cognate ligands. The cell line was kindly provided by Dr William Claycomb. Cells are grown in complete supplemented Claycomb media (JRH Biosciences, Lenexa, Kansas). Stimulations and transfections are performed with the cells at confluence.

Primary murine cardiomyocytes: Murine ventricular myocytes are isolated from 10-14 week old adult male mice. After pelleting, cells are suspended in AS media (Cellutron, Highland Park, NJ) at a density of 20,000 cells/mL and placed in a 37^{o}C incubator on matrigel (BD Biosciences, Franklin Lakes, NJ) coated coverslips. When cells are to be kept in culture greater than 8 hours 10 mM 2,3–butanedione monoxime is added to the media.

Genetically engineered mice: MyD88 knockout mice were obtained from S Quereshi (Montreal PQ). NF-κB knockout mice (NF-kB KO 129P-Nfkb1tm1Bal/J) were obtained from Jackson Labs. Genotype was verified through RT-PCR.

Cell culture treaments: 10ug/mL E. Coli LPS (Invivogen, San Diego CA) is added 4 hours prior to harvesting cells for RNA assays and, in separate experiments, 24 hours prior to harvesting supernatant for protein assays. Inhibition of RAGE**:** 1ug/ml anti-

murine RAGE blocking antibody (R&D Systems, Minneapolis MN) was added to supplemented Claycomb media + 10% FBS 24 hours prior to calcium flux measurement.

Plasmids and transfections: Lipofectamine 2000 in OPTIMEM (Invitrogen, Carlsbad, CA) is used as per the manufacturer's instructions. S100A8 and S100A9 vectors (Origene Technologies, Rockville, MD) and mock transfection using the backbone only is performed. We have found that transfection efficiency, as determined using a GFP containing plasmid, is 50-60% at 48 hours. S100A9 siRNA plasmid and control/scrambled siRNA plasmid (Sigma, Oakville Canada) were used in vivo only.

Luciferase assay: HL-1 cells were transfected as above using pNFkB-Luc vector (BD Biosciences, Franklin Lakes, NJ) and a Renilla pGL4.74 [hRluc/TK] vector (Promega, Madison, WI). Cells were lysed using Passive Lysis Buffer (Promega), then luminescence quantified using the Dual-Luciferase Reporter Assay (Promega #1910) and a Fluostar Optima Luminometer (BMG Labtech, Durham NC). Relative Light Units (RLU) were obtained for both Renilla and the Firefly Luciferase and all results expressed as the ratio of Luciferase RLU to Renilla RLU.

Immunoprecipitation and immunoblotting: Tissues and cells were were homogenized in cell lysis buffer containing protease inhibitors aprotinin 10 ug/uml and leupeptin 10ug/ml and the phosphatase inhibitor sodium orthovanadate 10 mM. Anti-S100A8 and anti-s100A9 (R&D Systems, Minneapolis MN), anti-RAGE (R&D Systems, Minneapolis MN) and anti-SERCA2A (Santa Cruz Biotech, Santa Cruz California) were used as

primary antibodies. Immunoprecipitation was performed with 1ug/ml anti-S100A8, S100A9 or isotype control Ab using the protein G immunoprecipitation kit (Roche, Laval PQ) as per the manufacturer's instructions.

Calcium flux assay: HL-1 cells grown to confluence on 4-well LabTek coverslips chambers (Sigma, Oakville, ON) are incubated for 30 minutes with 2.5 uM Fura-2 calcium-gated fluorescent dye (Molecular probes). Fluoresence is captured using a photomultiplier detector (Ionoptix corp, Milton, MA) and analyzed using an Ionoptix Softedge detection package that directly yields dynamic cardiomyocyte calcium flux (Ionoptix corp, Milton, MA). Calcium flux is calculated as peak to baseline difference in the ratio of emissions from excitation wavelengths 340/380 nm.

RNA extraction and quantitative RT-PCR: Total RNA is extracted using Trizol (Invitrogen, Carlsbad, CA) as per the manufacturer's instructions. 1 μg of RNA is treated with DNAase I Amplification Grade (Invitrogen, Carlsbad, CA). One step Quantitative real time RT-PCR will be performed using a SYBR green RT-PCR kit (QIAGEN Inc. Mississauga, ON) according to manufacture's instructions on an ABI 7200 detection system (Applied Biosystems, Foster City, CA). 20 μL samples are amplified using a program that includes a reverse transcription procedure consisting of one cycle at 50℃ for 30 minutes and 95℃ for 15 minutes followed by 40 cycles of denaturation step at 94 ℃ for 15 seconds, annealing step at 60℃ for 30 seconds and extension step at 72℃ for 30 seconds. The absolute amount of the target gene is determined using external

standards. S100A8 and S100A9 primers were obtained from ABI's list of pre-validated primer-probe sets (Applied Biosystems, Foster City, CA).

Cardiac-specific gene delivery: Depot microbubbles (Visualsonics, Toronto ON) 5uM in diameter are reconstituted with 2ug/ul endotoxin-free plasmid and incubated 30 minutes at room temperature. 4ul/gram of this plasmid-microbubble mixture is injected via mouse tail vein. Successful injection is confirmed through echocardiographic visualization with the Vevo 770 small animal ECHO (Visualsonics, Toronto ON) of contrast first in the right ventricular cavity then within 3 cardiac cycles the left ventricular cavity. Ten minutes following intravenous injection ventricular tissue opacification due to capillary lodging of the microbubbles is maximum while intravascular contrast has largely cleared. Microbubbles are then cavitated using 4 pulses per level of the low-frequency/high-energy "destruct" mode within the contrast software mode (Visualsonics, Toronto ON). This destruction is performed at levels from cardiac base to apex.

Echocardiographic assessment of mice: Mice are lightly anesthetized with 1-3% inhaled isofluorane and placed on a warming blanket. M-mode echocardiograms are targeted from 2D echos obtained using the Vevo 770 ECHO (Visualsonics, Toronto ON) operating at a 120 Hz frame rate. Left parasternal 2D left ventricular cross-sectional echocardiographic images are obtained. The position and angle of the echo transducer is maintained by directing the beam just off the tip of the anterior leaflet of the mitral valve and by maintaining internal anatomic landmarks constant. All measurements are taken from M-mode traces at end-expiration. Left ventricular internal dimensions will be

measured at end-diastole (defined as the onset of the QRS complex in lead II of the simultaneously obtained electrocardiogram) and at end-systole (defined as minimum internal ventricular dimension).